EXOSKELETONS

The role of user preference in the customized control of robotic exoskeletons

K. A. Ingraham[1,2], C. D. Remy[3], E. J. Rouse[1,2]*

User preference is a promising objective for the control of robotic exoskeletons because it may capture the multifactorial nature of exoskeleton use. However, to use it, we must first understand its characteristics in the context of exoskeleton control. Here, we systematically measured the control preferences of individuals wearing bilateral ankle exoskeletons during walking. We investigated users' repeatability identifying their preferences and how preference changes with walking speed, device exposure, and between individuals with different technical backgrounds. Twelve naive and 12 knowledgeable nondisabled participants identified their preferred assistance in repeated trials by simultaneously self-tuning the magnitude and timing of peak torque. They were blinded to the control parameters and relied solely on their perception of the assistance to guide their tuning. We found that participants' preferences ranged from 7.9 to 19.4 newton-meters and 54.1 to 59.2 percent of the gait cycle. Across trials, participants repeatably identified their preferences with a mean standard deviation of 1.7 newton-meters and 1.5 percent of the gait cycle. Within a trial, participants converged on their preference in 105 seconds. As the experiment progressed, naive users preferred higher torque magnitude. At faster walking speeds, these individuals were more precise at identifying the magnitude of their preferred assistance. Knowledgeable users preferred higher torque than naive users. These results highlight that although preference is a dynamic quantity, individuals can reliably identify their preferences. This work motivates strategies for the control of lower limb exoskeletons in which individuals customize assistance according to their unique preferences and provides meaningful insight into how users interact with exoskeletons.

INTRODUCTION

The newest-generation lower-body exoskeletons are high-performance, untethered, and lightweight (*1*–*4*) but have not yet achieved adoption as devices to augment able-bodied ambulation. One barrier to translation is that designing effective control systems for such devices is challenging due to the complexity of interfacing directly with the human body. For exoskeletons to achieve their full potential as augmentative devices, the robotic assistance must provide a benefit to the user while also synergistically integrating with the user's neuromotor system. Fundamental to the realization of this vision is the definition of appropriate efficacy criteria, or objectives, for exoskeleton assistance. This is currently a rich field of study, yet the optimal objectives for able-bodied augmentation remain unknown. To accelerate the translation of robotic exoskeleton systems, it is imperative that control system designers analytically investigate metrics that capture a broad spectrum of relevant outcomes associated with exoskeleton use. Furthermore, to enable synergistic human-robot interaction, we must expand our definition of optimality and consider not only how robotic assistance affects biomechanical elements of gait but also how individuals perceive, interact with, and learn from the assistance.

In many state-of-the-art exoskeleton control systems, a desired objective is maximized through the tuning—or optimization—of the controller architecture and associated parameters. Commonly, controllers for lower limb exoskeletons command parameterized assistance (such as joint torque or power) as a function of time (*2*), presumed location in the gait cycle (*5*–*9*), or muscle activity (*10*). The choice of the controller parameterization and the subsequent parameter tuning not only govern the behavior of the robot but also markedly affect the user's walking mechanics and energetics (*5*, *7*–*9*) and experience wearing the device (*11*). Although various objectives for lower limb exoskeleton assistance have been explored (*12*), by far the most common physiological objective for able-bodied augmentation has been to reduce the metabolic cost of the user (*4*). A promising technique to minimize the user's energy cost is known as human-in-the-loop optimization (*13*–*17*). In this paradigm, the user performs a continuous activity, such as walking on a treadmill, while an online optimization algorithm iteratively modifies characteristics of the exoskeleton's assistance profile to arrive at the optimal settings. A real-time estimate of the user's metabolic cost serves as the cost function that the algorithm seeks to minimize (*18*). Recent experiments have demonstrated that human-in-the-loop optimization has the potential to yield large energetic savings while wearing an exoskeleton with optimized control settings compared with unassisted walking (*13*, *16*). However, human-in-the-loop optimization methods are currently limited by their reliance on one, predefined, measurable physiological objective as a metric of device efficacy.

In reality, users may prioritize any number of different metrics simultaneously while wearing a robotic exoskeleton, such as comfort, stability, pain, symmetry, or perceived effort. Thus, current controller optimization techniques based solely on minimizing energy expenditure omit valuable information. However, it is challenging to design a control system based upon subjective quantities. Even if it were possible to robustly measure such metrics, we would not know how to properly assign weights to the discrete metrics to meet an individual user's needs. Alternatively, asking users about their preference may inherently encode relevant information from multiple sources related to the user's experience. With user preference as an objective function for exoskeleton control optimization,

[1]Department of Mechanical Engineering, University of Michigan, Ann Arbor, MI, USA. [2]Robotics Institute, University of Michigan, Ann Arbor, MI, USA. [3]Institute for Nonlinear Mechanics, University of Stuttgart, Stuttgart, Germany.
*Corresponding author. Email: ejrouse@umich.edu

the potential emerges for individuals to customize the device assistance according to their own criteria for optimality. In this paradigm, the user performs their own optimization internally, which eliminates the burden on researchers to identify, measure, and assign individual weights to the myriad unknown elements that comprise optimal exoskeleton assistance.

In addition to its role as a target for controller optimization, user preference may also be used to promote synergistic human-robot interaction. Current exoskeleton controllers with the human "in the loop" measure physiological signals (such as muscle activity or metabolic cost) to inform the assistance generation, but this type of shared-control paradigm is unidirectional—the wearer has no conscious control over the assistance provided by the device. Researchers across many fields of assistive and rehabilitation robotics have demonstrated that bidirectional interaction is generally preferred by users and that high levels of user satisfaction are required for the acceptance of autonomous robotic assistance (*19*–*23*). However, control sharing is a relatively nascent field when applied to robotic exoskeleton technology (especially for able-bodied augmentation), and it is not yet known which types of control sharing paradigms may be appropriate. To address this challenge, it is important to understand the characteristics and temporal features of user preference, such as how quickly and reliably users can identify their preferences or how preference changes over time. Understanding these facets of preference may provide practical benchmarks for implementing future shared-control frameworks.

To use preference as an optimization criterion for lower limb exoskeletons, it must be robustly measured, and we need to understand how it changes as individuals adapt to the assistance. Recent studies have investigated users' preferences in assistance provided by lower limb prostheses (*24*–*30*) and exoskeletons (*11*, *31*–*34*). To measure preference, some studies used a forced choice paradigm, in which participants were presented with pairwise comparisons (A-B testing) (*29*, *31*–*33*) or asked to compare a condition to their own internalized preference (*24*, *25*). Data obtained from such methods can be used to identify or learn a user's preference, but it may require extended experimental time to obtain enough comparisons. As an alternative to forced choice methods, some studies used a method of adjustment, in which individuals adjusted control parameters until they achieved their preferred assistance (*26*–*28*, *30*, *34*). Such "self-tuning" methods are advantageous because they can quickly yield an individual's preference and are intuitive to the user—it is easy to imagine someone using a smart phone or watch to adjust their settings during activities of daily living. Previous studies have demonstrated success using self-tuning to identify individual preferences in one dimension (*26*, *27*), yet it is an open question how to extend these methods to multiple dimensions. One option is to perform one-dimensional sweeps through each parameter sequentially (*28*), but this method is time consuming and does not allow participants to assess how potential interactions between parameters affect their preference. Prior studies have laid the foundation for the robust measurement of user preference, yet to our knowledge, no studies have investigated how user preference changes as individuals adapt to robotic assistance.

Incorporating user preference into exoskeleton control systems has the potential to increase user satisfaction, promote acceptance, and add a rich source of information that cannot be easily measured using standard biometric sensors. Yet, preference-based control for lower limb exoskeletons is a relatively new research area, and we must first answer fundamental questions about user preference in the context of exoskeleton control. The goal of this study was to measure users' preferences in the applied torque characteristics of bilateral robotic exoskeletons and characterize how preference varies with walking speed, device exposure, and prior technical knowledge. We developed a two-dimensional grid interface that allowed participants to explore different settings in real time and identify their preferred assistance. Individuals were presented with a blank grid with changing axes, and they were not given any information about the control system parameters—the only instruction they were given was "find your preference." This paradigm ensured that participants relied upon their perception of the robotic assistance to guide their tuning and enabled us to systematically characterize trends in users' preferences across repeated trials.

In this study, 24 nondisabled participants (12 naive and 12 knowledgeable exoskeleton users) wore bilateral robotic ankle exoskeletons and self-tuned two parameters of the device's applied torque profile to identify their preferred assistance (Fig. 1 and figs. S1 and S2). Here, we analyze participants' preferred assistance parameters, how precisely they identified their preferences across repeated trials, and the strategies they used to find their preferences. We found that several features of participants' preferences, precision, and exploration strategies varied with walking speed or time spent using the device, as well as between naive and knowledgeable exoskeleton users. This work demonstrates that individual users have unique preferences in their exoskeleton assistance that they can quickly and reliably identify. These results inform the design of preference-based control strategies for lower limb exoskeletons and provide meaningful insight into how users interact with exoskeleton assistance.

RESULTS

Individuals reliably identified unique preferences in characteristics of their robotic exoskeleton assistance

To identify their preferred exoskeleton assistance parameters, participants were presented with a blank two-dimensional grid displayed on a touch screen tablet (Fig. 1B). Touching the grid instantaneously changed the torque profile the user experienced by commanding the magnitude and the timing of peak torque (Fig. 1C). Participants were instructed to explore the grid before deciding on their preference (Fig. 1D). The naive cohort (who had no prior exoskeleton experience) performed three blocks of eight preference-identification trials, for a total of 24 trials. The participant's walking speed (1.0, 1.2, or 1.4 m/s) varied between trial blocks, and we block-randomized the presentation of speeds.

Across all trials, naive participants' preferred magnitude ranged from 7.9 to 19.4 Nm (Fig. 2A), or 95% of the explorable range. As a metric of participants' precision across trials, the mean (SD) within-participant standard deviation of preferred magnitude was 1.7 (0.7) Nm, or 13.2% of the explorable range. As a metric of the variability between participants, the between-participant standard deviation of preferred magnitude was 3.7 Nm (2.1 times the within-participant standard deviation). There was no correlation between preferred magnitude and body mass (Pearson's correlation coefficient, $r = 0.13$) or height ($r = 0.31$) (fig. S3).

Across all trials, naive participants' preferred timing ranged from 54.1 to 59.2% gait cycle (Fig. 2A), or 50% of the explorable range. The mean (SD) within-participant standard deviation of preferred timing was 1.5 (0.7) % gait cycle, which corresponds to 12.5% of the explorable range. The between-participant standard deviation of

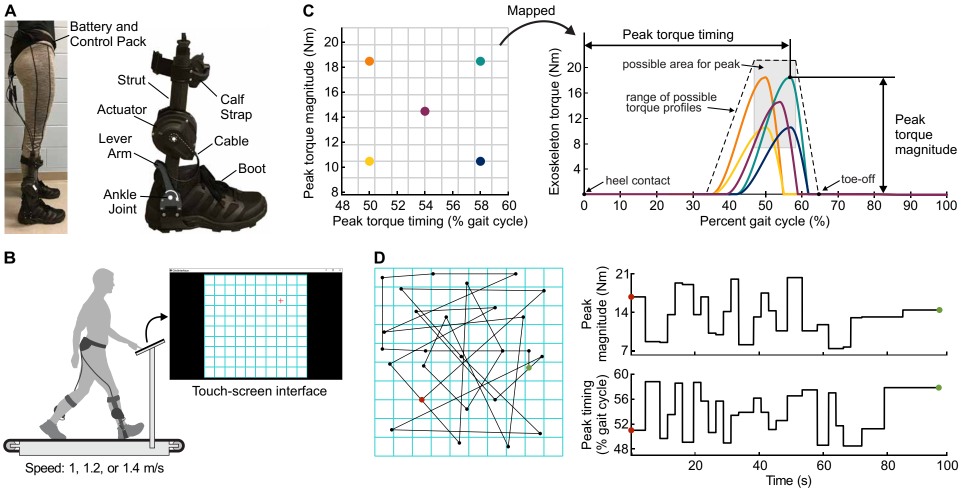

Fig. 1. Bilateral ankle exoskeletons and preference-identification protocol. (**A**) Bilateral ankle exoskeleton (Dephy). (**B**) Participants self-tuned their exoskeleton controller using a blank two-dimensional grid displayed on a touch screen tablet mounted to the treadmill. (**C**) Touching the grid instantaneously changed the torque profile that the user experienced by commanding the peak torque magnitude and timing. The axes of the grid were hidden from the participant but are shown here to illustrate the mapping between the parameter coordinates and corresponding torque profiles. The gray shaded area indicates the location of the peak torque that individuals could achieve within the limits of the grid; the black dashed line encompasses the corresponding range of torque profiles. (**D**) A representative preference-identification trial. Participants explored a blank two-dimensional grid, beginning at a random initial condition (red circle) and ending at their preferred settings (green circle). Black circles indicate the settings the participant sampled. Black lines connect settings in the order they were explored; these lines were added for visualization and did not appear on the participant's screen. The corresponding time-series representations of the participant's exploration are also shown.

preferred timing was 1.5% gait cycle (1.0 times the within-participant standard deviation). There was no correlation between preferred timing and body mass ($r = -0.21$) or height ($r = -0.08$) (fig. S3).

Across all trials, naive participants sampled 21.5 (SD: 6) settings and explored for 104.9 (34.2) s before confirming their preference. On average, participants took 4.3 (1.0) strides and spent 4.8 (1.3) s per setting before changing to a new setting.

Individuals' preferred torque magnitude increased as the experiment progressed

We analyzed the effects of speed and trial block on naive participants' preference using linear mixed-effects models (LMEMs). There was a significant effect of trial block on preferred magnitude (LMEM; $P = 0.03$) (Fig. 3B). From the slope of the model, we estimate that a participant's preferred magnitude would increase by 1.5 Nm from the first to the last trial block (Table 1). We additionally observed a mild positive relationship between preferred magnitude and walking speed (LMEM; $P = 0.19$) (Fig. 3A). Participants' preferred timing did not vary with speed (LMEM; $P = 0.88$) (Fig. 4A) or trial block (LMEM; $P = 0.56$) (Fig. 4B).

Individuals were more precise at identifying their preferred torque magnitude at faster walking speeds

We analyzed the effects of speed and trial block on naive participants' precision. The standard deviation of participants' preferred magnitude significantly decreased (participants became more precise) as walking speed increased (LMEM; $P = 0.03$) (Fig. 5A). From the slope of the model, we estimate that a participant's standard deviation of preferred magnitude would decrease by 0.5 Nm as walking speed increased from 1.0 to 1.4 m/s (Table 1). The standard deviation of participants' preferred magnitude exhibited a decreasing trend with respect to trial block (LMEM; $P = 0.16$) (Fig. 5C). For the standard deviation of preferred timing, we observed a trend toward increased precision with increasing speed (LMEM; $P = 0.14$) (Fig. 5B). The standard deviation of preferred timing did not vary with trial block (LMEM; $P = 0.98$) (Fig. 5D).

Individuals became more efficient at identifying their preferences as the experiment progressed

We analyzed the effects of speed and trial block on naive participants' exploration strategies. Trial block had a significant effect on all four exploration strategy outcomes (Table 1). The models predicted that from the first to the last trial block, participants would explore 6.6 fewer settings (LMEM; $P = 0.03$) (Fig. 6E), reduce total exploration time by 57.4 s (LMEM; $P < 0.001$) (Fig. 6F), take 0.9 fewer strides per setting (LMEM; $P = 0.001$) (Fig. 6G), and reduce time per setting by 1.0 s (LMEM, $P < 0.001$) (Fig. 6H).

Walking speed had a significant effect on the number of strides per setting (LMEM; $P < 0.001$) (Fig. 6C), and the model predicted that increasing speed from 1.0 to 1.4 m/s corresponded to 0.6 more strides per setting (Table 1). With increasing walking speed, we observed a trend toward fewer settings explored (LMEM; $P = 0.08$) (Fig. 6A) and shorter exploration time (LMEM; $P = 0.07$) (Fig. 6B). Increasing speed did not affect the time per setting (LMEM; $P = 0.60$) (Fig. 6D).

Individuals with prior exoskeleton knowledge or experience preferred higher torque magnitude

The knowledgeable cohort (who had prior exoskeleton knowledge or experience) performed a shortened protocol and completed one block of eight preference-identification trials walking at 1.2 m/s. We compared preference and precision outcomes between the naive and knowledgeable cohorts during the speed-matched condition (1.2 m/s). Knowledgeable participants preferred 3.8 Nm higher torque magnitude than naive participants (t test, $P = 0.03$, Cohen's $d = 1.06$) (Fig. 7A). We did not detect differences between groups in their preferred timing (t test, $P = 0.71$, $d = 0.15$) (Fig. 7B), standard deviation of preferred magnitude (t test, $P = 0.57$, $d = 0.45$) (Fig. 7C), or standard deviation of preferred timing (t test, $P = 0.49$, $d = 0.28$) (Fig. 7D).

DISCUSSION

Participants identified unique preferences (Fig. 2), which corroborates mounting evidence that optimal exoskeleton assistance requires individualized tuning. We observed several important factors related to the preferred characteristics of ankle exoskeleton

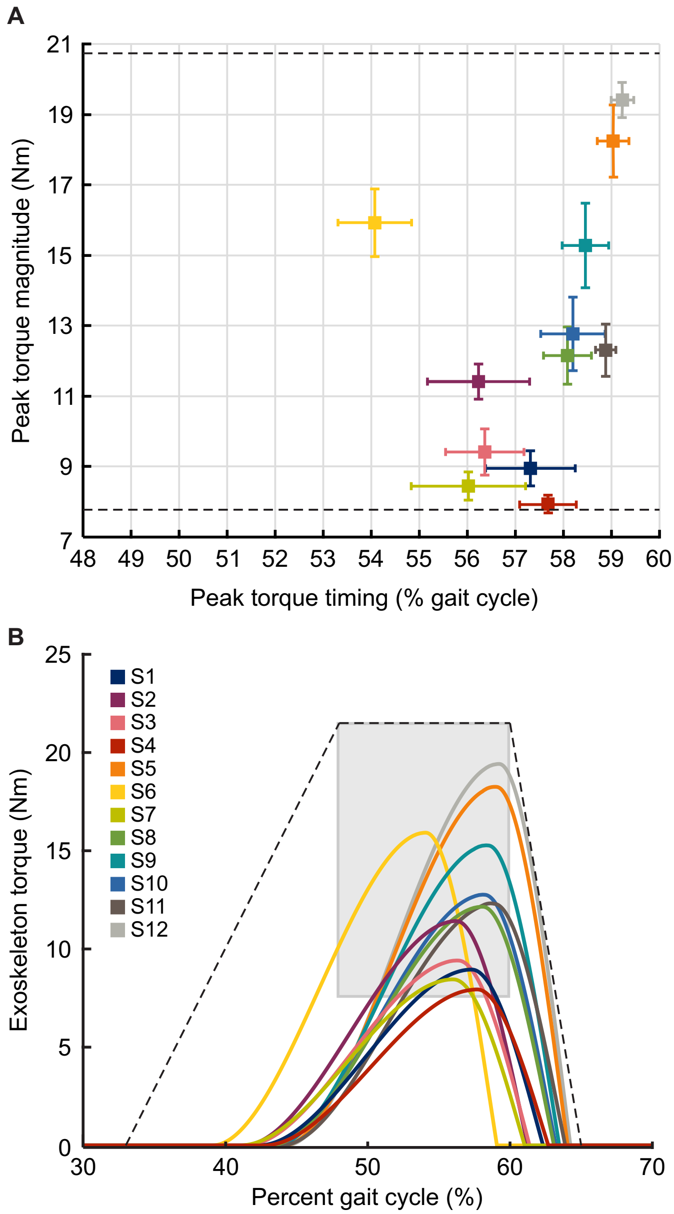

Fig. 2. Naive participants' preferred exoskeleton assistance. (**A**) Participants' mean preferred magnitude and timing across all 24 preference-identification trials. Colored squares and error bars depict the mean and 95% confidence interval for each parameter. The black dashed lines indicate the approximate bounds of torque magnitude that individuals could explore using the touch screen. (**B**) Participants' preferred torque profiles corresponding to their mean preferred parameters. The gray shaded area depicts the location of the peak torque that individuals could achieve using the touch screen; the black dashed lines encompass the corresponding range of torque profiles. Please note that the *x* axis displays 30 to 70% gait cycle to better visualize individual profiles. For reference, the peak biological ankle torque achieved during treadmill walking at similar speeds is about 100 Nm (*35*).

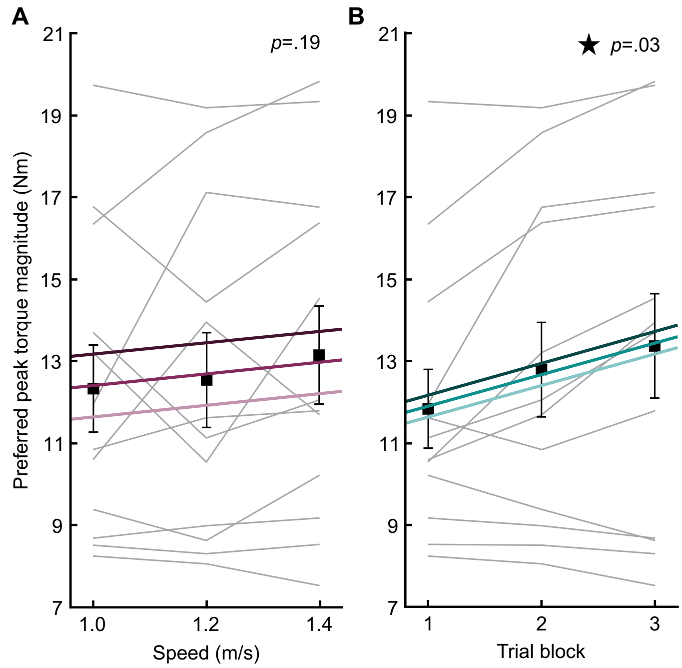

Fig. 3. Preferred peak torque magnitude as a function of speed and trial block. (**A**) Preferred magnitude as a function of walking speed. Purple lines show the slope of the LMEM with respect to walking speed and depict the expected outcomes for trial block 1 (light), block 2 (medium), and block 3 (dark). (**B**) Preferred magnitude as a function of trial block. Teal lines show the slope of the model with respect to trial block and depict the expected outcomes for speeds of 1.0 m/s (light), 1.2 m/s (medium), and 1.4 m/s (dark). Black squares and error bars represent the interparticipant mean and SEM. Gray lines connect individual participants' means (over eight trials) for each speed or trial block. The *P* value for each fixed-effect parameter estimate appears at the top of each panel; a black star indicates $P < 0.05$.

assistance. First, participants' magnitude preferences were distributed over 95% of the range of explorable settings. Most participants preferred to feel the exoskeleton assisting them to some degree and did not choose to eliminate the assistive torque. The exception to this may be participant 4 (who repeatedly selected the lowest torque setting available on the screen), but because we did not allow exploration below ~7.8 Nm, we cannot say whether this individual would have preferred lower torque if it had been available to them. Similarly, individuals did not repeatedly seek the maximum device assistance, which indicates that for this device, the range of exoskeleton torque provided in this study was inclusive of most participants' preferences. Last, preferred magnitude did not scale with body mass or height (fig. S3). Unlike magnitude, participants' timing preferences fell within a narrower band, and all but one of the participants' preferences were concentrated between 56 and 59% gait cycle. This range of 3% gait cycle corresponds to 33 ms, or only 6% of stance phase. These results demonstrate that individuals have an internalized representation of how they wish to receive exoskeleton assistance.

Individuals demonstrated their ability to precisely identify their preferences in two dimensions simultaneously, while navigating the interface relying solely on their perception of device assistance. Across naive participants, the mean standard deviation of preferred timing (1.5% gait cycle) corresponds to just 17 ms for the average stride time observed in this study. This variability is comparable with the mean stride-to-stride variability for the timing of biological peak ankle torque during treadmill walking, which is 0.9 to 1.5% gait cycle for speeds between 1 and 1.4 m/s (*35*, *36*). The mean standard deviation of preferred magnitude (1.7 Nm) represents 1.7% of the average peak

Table 1. Results from LMEMs for each outcome with speed and trial block as fixed effects. Bold text indicates a significant effect with $P < 0.05$.

	Outcome	Fixed effect = speed (tested range 1–1.4 m/s): Fixed effect parameter estimate [95% CI]	Fixed effect = speed: P value†	Fixed effect = speed: Expected change over tested range* (0.4 m/s)	Fixed effect = trial block (tested range 1–3): Fixed effect parameter estimate [95% CI]	Fixed effect = trial block: P value†	Fixed effect = trial block: Expected change over tested range* (2 blocks)
Preference outcomes	Preferred magnitude (Nm)	1.33 [–0.07, 2.72]	.19	0.53	**0.77 [0.21, 1.33]**	**.03**	**1.54**
	Preferred timing (% gait cycle)	–0.54 [–1.90, 0.82]	.88	0.21	–0.11 [–0.48, 0.26]	.56	–0.22
Precision outcomes	Std. dev. of preferred magnitude (Nm)	**–1.26 [–2.14, –0.38]**	**.03**	**–0.05**	–0.17 [–0.35, 0.003]	.16	–0.35
	Std. dev. of preferred timing (% gait cycle)	–1.26 [–2.62, 0.10]	.14	–0.50	0.00 [–0.28, 0.27]	.98	–0.01
Exploration strategy outcomes	Number of settings explored (# settings)	–7.51 [–14.07, –0.94]	.08	–3.00	**–3.30 [–5.67, –0.93]**	**.03**	**–6.60**
	Exploration time (s)	–38.17 [–73.57, –2.78]	.07	–15.27	**–28.68 [–41.11, –16.26]**	**< .001**	**–57.36**
	Number of strides per setting (# strides)	**1.48 [0.76, 2.20]**	**< .001**	**0.59**	**–0.42 [–0.64, –0.20]**	**.001**	**–0.85**
	Time per setting (s)	0.21 [–0.58, 1.00]	.60	0.08	**–0.51 [–0.75, –0.28]**	**< .001**	**–1.03**

†*P* values have been adjusted using family-wise Holm-Bonferroni correction. *Expected change was calculated by multiplying the parameter estimate by the difference over the tested range (0.4 m/s or 2 blocks).

biological ankle torque observed during walking (*35*). This variability corresponds to only 20 to 40% of the mean stride-to-stride variability for the magnitude of biological peak torque during treadmill walking, which is 3.8 to 7.3 Nm for speeds between 1 and 1.4 m/s (*35*, *36*). It is important to note that these results may represent the lower bound of an individual's precision. In this study, participants were blinded to the control parameters and the axes were hidden and randomized between trials. In addition, the resolution of the touch screen and participant's finger size and ability to select a fixed target while walking on the treadmill may have further limited their fine-tuning capability. Experimental studies will be necessary to determine how the precision varies if participants are given feedback about their tuning choices and how it is influenced by features of the self-tuning interface.

Participants were also able to identify their preferred settings quickly, with an average exploration time of 1.8 min. Even if users needed to perform three to five repeated trials to obtain an average preference, the entire tuning procedure would take 5 to 10 min. This is faster than the pairwise comparison method used in (*31*), which required 20 trials for the algorithm to build an approximation of the user's preference in one dimension. Together, the speed and precision of participants' preference identification demonstrate that users are a reliable source of information, and that the two-dimensional self-tuning paradigm may be an efficient method for implementing preference-based exoskeleton control systems.

Participants did not prefer peak torque magnitude and timing parameters that replicated the biological ankle's peak torque as a function of treadmill speed. We observed only a mild trend between preferred magnitude and speed (Fig. 3A), and the effect was small. Our analyses predicted that preferred magnitude may increase by 0.5 Nm (95% confidence interval: 0.0 to 1.1 Nm, $P = 0.19$) as treadmill speed increases from 1.0 to 1.4 m/s, which corresponds to a 6.7% increase. From the literature, we estimate that the biological ankle's peak torque increases by about 14.3% over the same range of treadmill speeds (*35*). Therefore, the increase in preferred peak torque magnitude observed in our study is approximately half the expected increase in biological peak ankle torque during treadmill walking. With regard to timing, the peak timing that individuals preferred in this study (56 to 59% gait cycle) is considerably later in the gait cycle than the peak of the biological ankle torque, which falls in the range of 45 to 49% gait cycle (*35*, *37*). Preferred timing also remained constant with respect to speed (Fig. 4A). Analysis of a recently published dataset indicates that the timing of peak biological torque occurs about 1.2% gait cycle earlier when walking on a treadmill at 1.4 m/s, compared with 1.0 m/s (*35*). While an intuitive starting place for designing ankle exoskeleton assistance is to supplement the biological ankle by replicating its mechanics during walking (*38*, *39*), the observations from our study indicate that users' preferred peak torque magnitude and timing do not follow trends in the biological ankle's peak torque with increasing treadmill speed. This suggests that there are complex and potentially counterintuitive mechanisms driving user preference.

One of our key findings is that user preference is not a static quantity, and naive users' preferred magnitude increased as the experiment progressed (Fig. 3B). There are numerous potential explanations for this result, and we elaborate here on only some of the possibilities. Because our participants were healthy young adults and

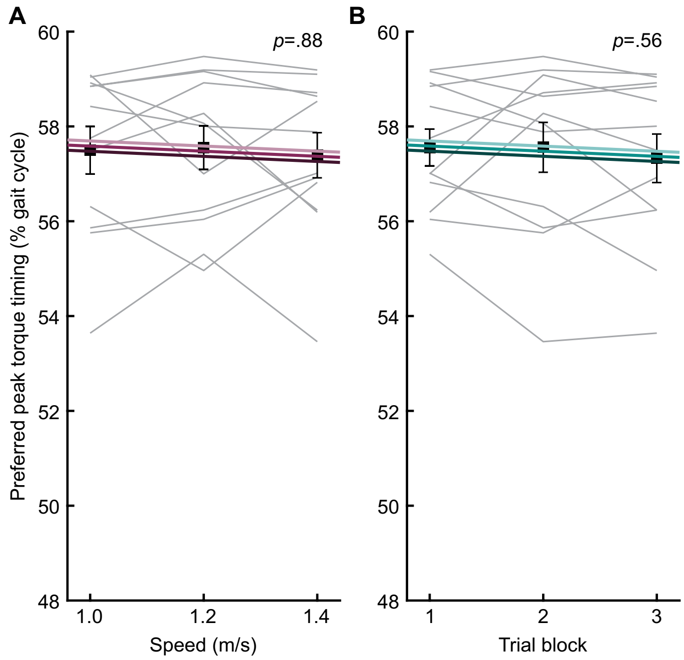

Fig. 4. Preferred peak torque timing as a function of speed and trial block. (**A**) Preferred timing as a function of walking speed. Purple lines show the slope of the LMEM with respect to walking speed and depict the expected outcomes for trial block 1 (light), block 2 (medium), and block 3 (dark). (**B**) Preferred timing as a function of trial block. Teal lines show the slope of the model with respect to trial block and depict the expected outcomes for speeds of 1.0 m/s (light), 1.2 m/s (medium), and 1.4 m/s (dark). Black squares and error bars represent the interparticipant mean and SEM. Gray lines connect individual participants' means (over eight trials) for each speed or trial block. The *P* value for each fixed-effect parameter estimate appears at the top of each panel; a black star indicates *P* < 0.05.

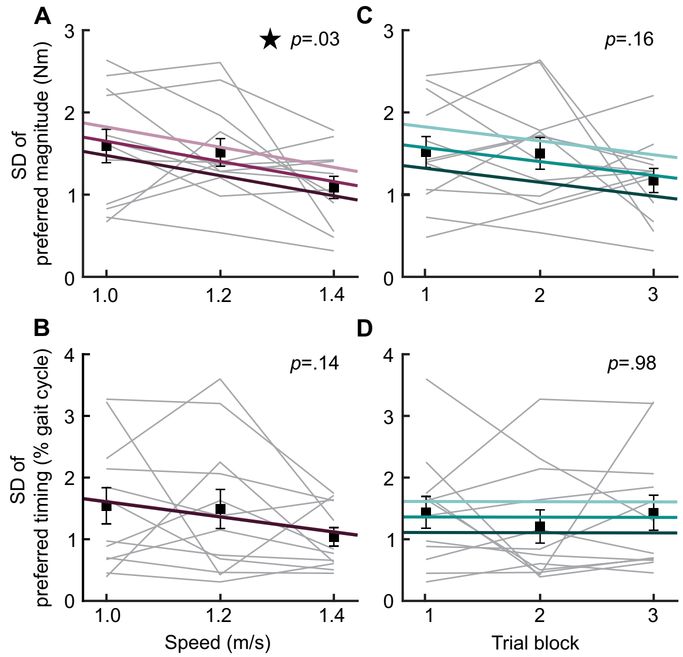

Fig. 5. Precision outcomes as a function of speed and trial block. (**A** and **B**) Standard deviation of preferred magnitude and preferred timing as a function of walking speed. Purple lines show the slope of the LMEM with respect to walking speed and depict the expected outcomes for trial block 1 (light), block 2 (medium), and block 3 (dark). (**C** and **D**) Standard deviation of preferred magnitude and preferred timing as a function of trial block. Teal lines show the slope of the model with respect to trial block and depict the expected outcomes for speeds of 1.0 m/s (light), 1.2 m/s (medium), and 1.4 m/s (dark). Black squares and error bars represent the interparticipant mean and SEM. Gray lines connect individual participants' means (over eight trials) for each speed or trial block. The *P* value for each fixed-effect parameter estimate appears at the top of each panel; a black star indicates *P* < 0.05.

walked for just 22 to 77 cumulative minutes [similar to (*13*, *16*)], with breaks every 1 to 3 min, we strongly believe that the effect is not a result of fatigue. Another possibility is that individuals discovered strategies to adapt their gait biomechanics to comfortably accept higher exoskeleton assistance. As one example, if individuals were initially destabilized by the exoskeleton assistance [as proposed in (*40*) and (*41*)] and thus preferred lower torque, they may have subsequently found gait strategies to accommodate higher torques while maintaining stability. Last, it is possible that a naive user's neuromotor system requires a certain duration of time and/or practice to adapt to exoskeleton assistance, and this adaptation manifests as changes in preferred torque magnitude. Support for this explanation may be found in previous studies demonstrating that biomechanical quantities (such as ankle kinematics and muscle activity) required 20 to 30 min to reach steady state in response to powered exoskeleton assistance (*42*, *43*). However, Cain *et al.* (*43*) also concluded that users' neuromotor adaptation changes depending on the control strategy used, so we cannot definitively extrapolate these results to our experiment. Because preference-based control for robotic exoskeletons is a relatively new research area, the time scale for a new user's preference adaptation has yet to be determined. Our study demonstrates that participants' preferred torque magnitude increases by 1.5 Nm over the course of 24 self-tuning trials (or 22 to 77 min of active exoskeleton use). These data may be used as a benchmark to determine how often a user might need to retune a preference-based exoskeleton controller or, alternatively, as motivation to design controllers with user preference continuously evaluated in the loop.

As the experiment progressed, in addition to preferring higher torque magnitude, participants also became more efficient at identifying their preferred magnitude. Examining changes in the participants' interaction with the self-tuning interface elucidates important elements related to how naive exoskeleton users learn to navigate the grid and identify their preferences. Participants' efficiency significantly increased as trial block increased, as quantified by all four exploration strategy metrics (Fig. 6, E to H) Simultaneously, we observed a moderate downward trend toward increased precision in preferred magnitude with respect to trial block (Fig. 5C). From a practical standpoint, participants likely developed strategies to navigate the grid interface more effectively with practice. Anecdotally, we observed that many participants streamlined their exploration strategy as the experiment progressed and converged to a "quadrant-based" strategy; participants would sample one to two settings from each quadrant of the grid, select the quadrant that felt best, and then fine-tune within the chosen quadrant (fig. S4). Our models revealed that, over the course of the experiment, participants would sample 6.6 fewer settings and explore for 57 fewer seconds before confirming their preference (Table 1), and we believe that it is reasonable to attribute these results to a more efficient exploration strategy. However, participants' increased efficiency and trend toward increased

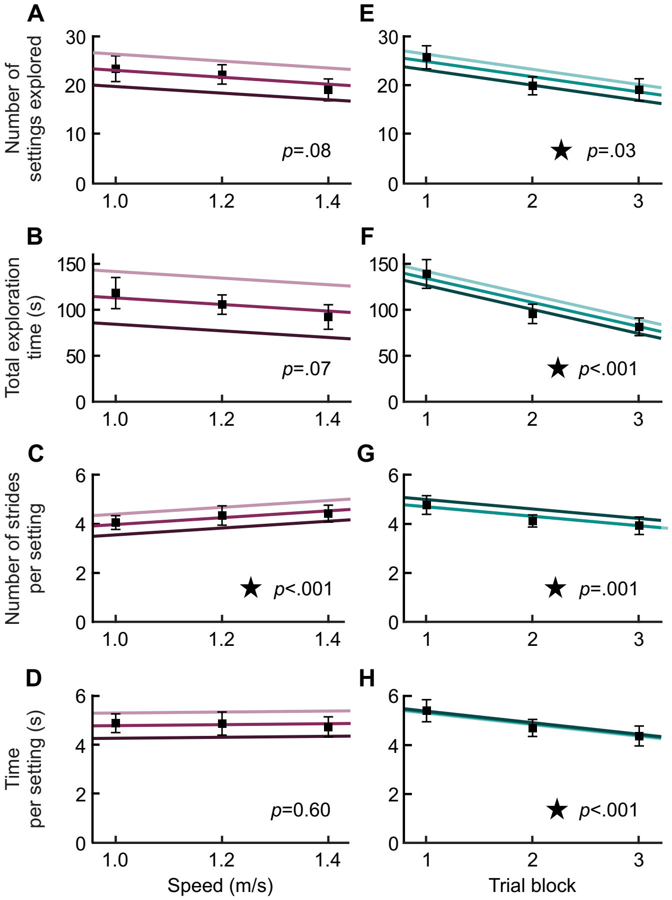

Fig. 6. Exploration strategy outcomes as a function of speed and trial block. (**A** to **D**) Four exploration strategy outcomes as a function of walking speed. Purple lines show the slope of the LMEM with respect to walking speed and depict the expected outcomes for trial block 1 (light), block 2 (medium), and block 3 (dark). (**E** to **H**) Four exploration strategy outcomes as a function of trial block. Teal lines show the slope of the model with respect to trial block and depict the expected outcomes for speeds of 1.0 m/s (light), 1.2 m/s (medium), and 1.4 m/s (dark). Black squares and error bars represent the interparticipant mean and SEM. The *P* value for each fixed-effect parameter estimate appears at the bottom of each panel; a black star indicates $P < 0.05$.

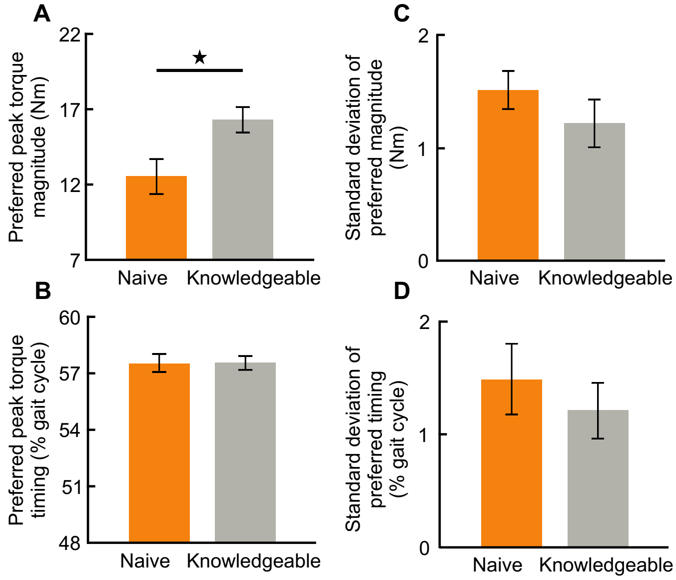

Fig. 7. Comparison of preference and precision outcomes between naive and knowledgeable users. (**A** and **B**) Interparticipant mean of preferred magnitude and timing for naive and knowledgeable cohorts walking at 1.2 m/s. (**C** and **D**) Interparticipant mean of the standard deviation of preferred magnitude and timing for naive and knowledgeable cohorts walking at 1.2 m/s. Black error bars show 1 SEM. A black bracket with a star indicates a significant difference between the means ($P < 0.05$), as calculated by a two-tailed *t* test.

precision could also point to adaptation in their perception of the exoskeleton assistance. Higher precision identifying their preferred magnitude may suggest that their ability to differentiate between similar magnitude settings improved or that they developed a more specific internal definition of their preference. An increased perceptual awareness may also be illustrated by examining the average number of strides individuals took at a given setting before selecting a new setting. Our analyses demonstrate that participants would take 0.9 fewer strides (and spend one less second) per setting in the third trial block compared with the first (Table 1). Therefore, as the experiment progressed, participants were able to make the same internal determination ("how does this feel, and do I like it?") at a particular setting more quickly, in approximately one fewer stride. At this time, we have not measured the human's perceptual ability to distinguish between characteristics of exoskeleton assistance (for example, the just noticeable difference), but quantifying this metric would aid in the interpretation of these results. From a control design perspective, these findings demonstrate that as participants gain experience using the device, they become more adept at searching for, and deciding upon, their preferred exoskeleton assistance.

An unexpected finding was that as walking speed increased, participants were significantly more precise in identifying their preferred magnitude (Fig. 5A), and we observed a moderate trend toward increased precision in identifying their preferred timing (Fig. 5B). These results are intriguing, especially considering that participants also trended toward increased efficiency (fewer settings explored and shorter exploration time) as speed increased, although these results were not statistically significant (Fig. 6, A and B). As the order of speeds a participant performed was evenly distributed within the participant pool, we do not believe that these are order effects. One possible explanation for the increased precision is that participants simply took more strides at faster speeds and therefore had increased exposure to the exoskeleton assistance. Participants did, in fact, take slightly more strides per setting at faster speeds (Fig. 6C), but did not spend more time per setting (Fig. 6D), which indicates that the increased stride count per setting is likely a result of faster treadmill belt speed. However, participants did not take more total strides per trial as speed increased. The average total number of strides taken per trial decreased monotonically with increasing walking speed, which may also explain the trend toward decreased total exploration time. Therefore, it does not seem that participants' increased precision with increased walking speed is attributable to more time spent walking or more total strides taken at faster speeds. An interesting hypothesis to explain these results is that an individual's "preference gradient" is steeper at faster walking speeds. In essence, this would mean that participants are more sensitive to the settings that feel good to them, and therefore select a more concentrated set of preferred settings. It could be that, at faster walking speeds, participants feel less stable or less comfortable at settings farther away from their preference. Alternatively, if individuals were more sensitive to the power delivered by the exoskeleton than the torque, they may be more precise in identifying their preferences in conditions with higher exoskeleton power, when the same torque burst is applied in concert with faster ankle angular velocity (*44*). The observed increase in precision at faster walking speeds is unexpected because the assistive torque (with a fixed width of 20% gait cycle) occurs over a shorter duration of time as walking speed increases and stride time decreases. This suggests that users are not only sensing the torque burst itself to decide on their preference, but they are actually evaluating the assistance over the entire gait cycle.

As discussed so far, user satisfaction and comfort are likely key elements that will affect the adoption of augmentation-focused exoskeleton technology in the future. Another critical piece may be user education surrounding the potential benefits of such devices. In this study, we observed that knowledgeable participants (who were researchers in the field of wearable robotics) preferred 3.8 Nm higher torque than the naive participants during the nominal speed condition (Fig. 7A). All participants were both read an identical script at the beginning of the experiment, so initial education did not bias our results. It is interesting that not all members of the knowledgeable cohort actually had prior experience walking using a powered exoskeleton, and there was no correlation between the previous number of hours spent walking using a robotic exoskeleton and preferred assistance settings (table S1). Therefore, we would not expect the knowledgeable participants' preferences to represent an asymptote of the naive participants' preferences as they gain walking experience. Rather, it appears that knowledgeable participants' experiences as researchers in the field primed them to prefer higher assistance from the exoskeleton. One possibility is that knowledgeable participants were more aware of the potential benefits of robotic assistance (energy cost reduction, for example) and thus preferred higher magnitudes. These findings speak to the importance of educating new users about the potential benefits of exoskeleton technology, because this knowledge may change the way the user interacts with the device and the assistance they prefer. For exoskeleton researchers, these results also expose the critical need to expand our recruitment pools beyond members of our research community—if we only perform experiments on knowledgeable individuals, we will likely miss out on important data indicating how naive users learn to use augmentative exoskeletons.

At this time, we can only speculate about why a participant selected their preferred settings or what quantities the individual may be seeking to optimize with their selection (such as energetics, stability, or comfort). In a recent study, Clites *et al.* (*30*) measured users' preferred stiffness of a custom ankle prosthesis while simultaneously recording anatomical, kinematic, kinetic, metabolic, and validated outcomes data to explore the relationships between preference and biomechanical and behavioral quantities. Their work demonstrated that kinematic symmetry may be a key correlate with user preference. Similar studies could examine such relationships in lower limb exoskeletons to understand what measurable quantities correlate with preference. In addition, collecting participant feedback through questionnaires or validated scales (such as the Borg Scale of Perceived Exertion) will help elucidate the factors driving an individual's preference selection. From a control design perspective, it is currently unknown how preferred control parameters differ from those selected by other tuning methods (such as human-in-the-loop optimization) and how using preference-based controllers corresponds to desirable biomechanical and energetic performance.

With our controller, we were limited to providing about 22 Nm of exoskeleton torque, which was the maximum we could reliably provide step-to-step without saturating the current limits of the device. While this is a relatively low amount of torque compared with similar studies (*13*, *38*), the maximum torque limit was high enough to capture all the naive participants' preferences. Because we were limited by the maximum torque we could provide, we had participants self-tune their torque magnitude in newton-meters (as opposed to the more common body-mass–normalized newton-meters per kilogram). This ensured that we did not need to reduce the maximum limit for heavier individuals. We performed the same analyses presented in this study using participants' normalized magnitude preferences (in newton-meters per kilogram), and the interpretation of our results did not change (Supplementary Text, figs. S5 to S7, and table S2). We did not measure exoskeleton torque directly but calculated it from the motor current, torque constant, and instantaneous transmission ratio. Given the high torque density of the actuator (*45*), the high efficiency of belt drives (*46*), and the low transmission ratio (15:1), we expect that the actual torque will be close to this estimated torque. Recent studies using exoskeletons with low transmission ratios (from 7:1 to 25:1) have demonstrated good agreement between estimated and actual torque (*3*, *47*–*49*), but this has not been experimentally validated for our system at this time. In addition, we periodically tightened the exoskeleton straps throughout the experiment to mitigate energy losses at the human-exoskeleton interface.

In this study, participants tuned two shaping parameters of the torque profile—peak torque magnitude and timing—while the rise time and fall time were held constant. Allowing participants to tune different parameter combinations would result in distinct exoskeleton mechanics (torque onset and offset times, total power), and it is not yet known how such characteristics influence users' preferences and precision. Participants performed one self-directed practice session (about 5 min) before performing the experimental trials, and we do not know how longer familiarization periods would affect the results. In addition, participants performed trials at fixed speeds instead of their self-selected speed, which may not be representative of how exoskeleton users would ambulate outside the laboratory. In this study, we compared the knowledgeable cohort with the naive cohort during their speed-matched condition (1.2 m/s), but we could have used the naive cohort's trial-matched condition (trials 1 to 8). We performed this additional analysis, and it did not change the observed differences between groups (Supplementary Text, fig. S8).

This foundational study establishes that users have unique preferences in their robotic ankle exoskeleton assistance and that they can precisely and quickly identify these preferences using a two-dimensional self-tuning interface. Because participants were blinded to the parameters they were tuning, this paradigm encouraged participants to customize the device assistance using their own perception and internalized representation of preferred device assistance. In conclusion, the results from this study demonstrate that robotic exoskeleton users are a reliable source of information related to their experience wearing the device. As such, we advocate for the inclusion of user preference in the design of future control systems—such systems may seek to optimize user preference or consider preference as one objective in a multi-objective optimization scheme, alongside other important performance metrics, such as energetics or biomechanics. Incorporating users' control preferences has the potential to promote synergistic human-robot interaction and accelerate the translation of augmentative exoskeleton systems.

MATERIALS AND METHODS

Study design

A cohort of 12 naive participants self-tuned the magnitude and timing of the assistive torque using a touch screen tablet (Fig. 1). We conducted repeated preference-identification trials at each of three walking speeds, presented in a block-randomized order. We quantified how individual preferences varied with both walking speed and time spent interacting with the device (trial block). Within this paradigm, we characterized how individuals searched for and identified their preferences and learned to use the tuning interface. Last, we investigated how prior knowledge of exoskeletons affected user preference. We repeated a shortened version of the self-tuning protocol at one speed with a cohort of 12 knowledgeable participants (researchers in the field of wearable robotics) and compared their preferences with those of the naive participants.

Participants

We recruited a naive cohort of 12 nondisabled participants (6 male and 6 female; mean age, 32.1 years; height, 1.77 m; weight, 78.6 kg) who had no prior experience walking using a robotic exoskeleton and were not researchers in the field of wearable robotics; this information was self-reported by participants on a questionnaire. We also recruited a knowledgeable cohort of 12 nondisabled participants (9 male and 3 female; mean age, 27.3 years; height, 1.77 m; weight, 69.0 kg) who self-identified on the questionnaire as researchers in the field of wearable robotics and reported from 0 to 100+ hours of walking using a robotic exoskeleton (table S1). Before data collection, all participants provided informed consent to a protocol approved by the University of Michigan Institutional Review Board. Individuals recruited for this study had no history of serious lower limb injury, had no neurological diseases affecting their movement or balance, and were not pregnant. Participants self-reported their gender, height, and age, and we measured their weight (table S1).

Ankle exoskeleton hardware

Participants wore bilateral ankle exoskeletons (Dephy Inc., Maynard, MA) (Fig. 1A and fig. S1). Each exoskeleton comprises an actuator, a boot, and a strut. The actuator (T-motor U8-KV100, Nanchang, Jiangxi, China) is a brushless motor that provides plantarflexion torque about the ankle joint by spooling an inelastic cable that is rigidly attached to a short lever arm on the boot. The lever arm is rigidly connected to a footplate embedded in the sole of the boot. The actuator is mounted to a strut, which is connected to the boot via the ankle hinge joint and affixed to the wearer's shank with an adjustable calf strap. Each exoskeleton has several onboard sensors: an absolute encoder at the ankle joint that measures ankle joint angle and velocity, an incremental encoder on the motor that measures motor angle and velocity, a current sensor that measures motor current, and an inertial measurement unit (IMU) that measures acceleration and angular velocity of the shank.

The exoskeleton geometry creates a nonlinear transmission ratio, which varies as a function of ankle angle. Using a benchtop test, we empirically characterized the exoskeleton's transmission ratio curve (the transmission ratio as a function of ankle angle) and represented this function as a fourth-order polynomial. Over the ankle angle's normative range of motion (40° plantarflexion to 20° dorsiflexion), the transmission ratio varies from 7:1 to 17:1, with a mean of 15:1 (fig. S9). A detailed description of the characterization procedure is provided in Supplementary Materials and Methods.

Participants wore a hip sack holding the lithium polymer batteries and the control microprocessor (Raspberry Pi 4, Cambridge, UK). In total, the bilateral device weighed 5 kg (boots: 1.1 kg; bilateral exoskeletons: 2.7 kg; battery and control pack: 1.2 kg). Before data collection, we fit each participant with the exoskeleton by selecting the properly sized boot, securing the calf straps and hip sack, and adjusting the posterior wires so that they did not hinder leg movement.

Ankle exoskeleton control

The exoskeleton controller prescribed exoskeleton torque as a function of stride percentage. The torque profiles were characterized by two shaping parameters: the magnitude of peak torque (newton-meters) and the timing of peak torque (percent gait cycle) (Fig. 1C). These torque profiles were designed using the methodology established by Zhang *et al.* (*13*), which generates polynomial coefficients that define the rising and falling portions of the exoskeleton torque as a function of stride percentage. A finite state machine governed the torque generation during each stride. The state machine had five states, and transitions between states occurred at set percentages of the stride (fig. S10). The total stride time used to calculate the current stride percentage was the average of the past three stride times, where stride time was measured from left heel contact to ipsilateral heel contact. We identified heel contact using shank angular velocity measurements from the on-board gyroscope. At subsequent heel contact (100% gait cycle), the mean (SD) phase error between calculated stride percentage and actual stride percentage was 0 (2.3) % gait cycle; the mean absolute phase error was 1.6%. As a first-order approximation, we assume that the phase error accumulates linearly with the gait cycle and estimate that the mean absolute phase error would be about 0.9% gait cycle, or 10 ms, at the average peak time observed in our study (57% gait cycle).

During states when the exoskeleton produced plantarflexion torque, we controlled the device using current control. At each time step, we calculated the current stride percentage and used the torque profile's polynomial coefficients to calculate the desired exoskeleton torque (*13*). Desired exoskeleton torque was converted to desired motor torque using the instantaneous transmission ratio (obtained using the transmission ratio curve and instantaneous ankle angle). Desired motor torque (T_m) was translated into desired current (i) using $i = T_m/k_t$, where k_t is the q-axis torque constant; for this motor, the torque constant was empirically determined to be 0.14 Nm/A (*45*). The commanded current was enforced on the device through a closed-loop current controller. We measured the exoskeleton torque by recording the delivered motor current and converting it back into torque using the inverse of the operations described above.

During the remaining states, which included early stance and swing phases, the desired exoskeleton torque was zero. In these states, the exoskeleton behaved "transparently" and exerted zero torque on the user while keeping the cable nearly taught so that the actuator was prepared to produce torque with minimal lag time. This was accomplished using position control to enforce the desired motor position. Further details about the implementation of the transparent controller can be found in Supplementary Materials and Methods.

Touch screen interface

To enable participants to manually tune their exoskeleton assistance settings in real time, we used a touch screen tablet (Microsoft Surface Pro 4, Microsoft Corporation, Redmond, WA) mounted to the treadmill (Fig. 1B). The touch screen displayed a blank two-dimensional grid (fig. S2). When the participant touched the screen, a small red crosshair appeared to indicate the current setting; previous settings remained on the screen as black crosshairs.

Touching the screen changed the assistance settings the participant experienced, beginning at the following left heel contact. Behind the scenes, the Cartesian coordinates of the two-dimensional grid were mapped to the parameter coordinates (magnitude and timing of peak torque) (Fig. 1C). To prevent the participants from returning to the same (x, y) location each trial, we created eight unique maps, in which the x and y axes corresponded to either peak torque magnitude or timing. Then, each axis was oriented either smallest to largest or largest to smallest, with respect to the origin. The map was hidden from the participants and randomized between trials. The presented map did not affect participants' preference or exploration strategy outcomes (fig. S11).

For peak torque magnitude, participants could explore from about 7.8 to 20.7 Nm. During pilot testing (*34*), we determined that 7.8 Nm was the approximate inflection point at which participants could begin to feel the exoskeleton assistance. Therefore, by setting the lower limit to 7.8 Nm, we ensured that participants could feel the exoskeleton assisting them at all locations of the grid. Because the peak commanded exoskeleton torque was not always the same as the peak measured exoskeleton torque, participants did not always experience the exact same boundaries of the grid. Across all participants and strides, the mean (SD) difference between the peak commanded torque and the peak measured torque was −0.005 (0.46) Nm; the mean absolute difference was 0.22 Nm. In this study, we report each participant's preferred magnitude in measured peak torque to capture what participants experienced when they chose their preferred settings.

For peak torque timing, the range of settings available to the participants was 48 to 60% gait cycle. The bounds for the timing parameter were selected from empirical testing and informed by the literature. For our exoskeleton and control system, timings earlier than 48% gait cycle were very uncomfortable for users and decreased their ability to walk normally. Yet, 48% gait cycle was low enough to capture the push-off timing that has resulted in reductions of metabolic cost below that of unassisted walking, as reported in previous studies (*13*, *38*). For both parameters, the grid was linearly interpolated on both axes between the minimum and maximum values over 74 points, resulting in a resolution of 0.17 Nm for torque magnitude and 0.16% gait cycle for torque timing.

Preference-identification protocol

Participants identified their preferred settings by self-tuning the magnitude and timing of the peak exoskeleton torque in real time using the touch screen interface. During a single preference-identification trial, participants began with a random assignment of one of the eight maps described in the previous section, and a randomized initial condition between 10.3 and 19.4 Nm and 50 and 57% gait cycle for magnitude and timing, respectively. Participants were read an initial script to educate them about the exoskeleton and communicate the goals of their task, which is provided in Supplementary Materials and Methods. Briefly, participants were instructed to explore the grid to find their preferred settings (Fig. 1D). When they found their preferred settings, they informed the experimenter, who stopped the trial. We verbally reminded participants to explore the space until they were confident in their preference but did not enforce any time limit on exploration.

Participants in the naive cohort performed three blocks of eight preference-identification trials, for a total of 24 trials. During each trial block, participants walked on a treadmill (Bertec, Columbus, OH) at 1.0 m/s (slow), 1.2 m/s (nominal), or 1.4 m/s (fast). The order of speeds presented was block-randomized within the participant pool, and two participants performed each of the six possible orders of speeds. Participants in the knowledgeable cohort performed one block of eight preference-identification trials at the nominal speed (1.2 m/s).

Before beginning the preference-identification trials, all participants performed a practice trial, during which they were allowed to explore the grid for as long as they wished to get used to the exoskeleton assistance. We encouraged participants to explore out to the edges of the grid to familiarize themselves with possible assistance settings they might experience during the experimental trials. On average, participants practiced walking with the exoskeletons for 4.1 (1.7) min [mean (SD) for 22 participants].

Data analysis

During each preference-identification trial, we recorded time series of all assistance settings and (x, y) coordinates participants experienced (Fig. 1D). We simultaneously recorded data from the exoskeleton, including motor angle, velocity, voltage, current, ankle angle and velocity, and shank angular velocity (figs. S12 and S13). At the termination of each trial, we noted the final settings corresponding to the participant's preference. We assessed eight outcomes in this study, divided into three categories: preference outcomes, precision outcomes, and exploration strategy outcomes. The two preference outcomes were preferred peak torque magnitude (newton-meters) and preferred peak torque timing (% gait cycle), which corresponded to the final settings the participant chose. The two precision outcomes were designed to assess participants' repeatability in identifying their preferred settings across trials. They were the standard deviation of preferred peak torque magnitude (newton-meters) and the standard deviation of preferred peak torque timing (% gait cycle). The four exploration strategy outcomes described how the participants performed the experiment and interacted with the touch screen. They included the number of settings an individual sampled before confirming their preference, the total exploration time before confirming their preference (seconds), the average number of strides taken per setting before changing to a new setting, and the average time spent per setting (seconds).

Statistics

Using data collected from the naive cohort (performing eight trials at each of three speeds), we built eight LMEMs, one for each outcome (*50*). Each base model included walking speed and trial block as fixed effects and a random intercept per participant. We determined the random effects structure for each model using a manual forward selection process based on the Akaike information criterion (AIC). We iteratively added random effects of participant-specific slopes for speed and trial block. If the model with the lowest AIC included more random effects than the base model, we compared that model with the model with the next-lowest AIC using a likelihood ratio test. If the likelihood ratio test was not significant ($P > 0.05$), we chose the model with the fewer number of predictors. A detailed description of the optimized model structures (including the number of exemplars) can be found in Supplementary Materials and Methods. We investigated including an interaction effect for speed and trial block in the models, and none of the optimized models had a significant interaction term (table S3). Thus, for simplicity, we present the models without the interaction effect.

Because each of the eight LMEMs produced two fixed effects parameter estimates, or slopes, with an associated P value, there were 16 P values evaluated for significance. We divided the eight outcomes into three theoretically informative families (preference outcomes, four statistical tests; precision outcomes, four tests; exploration strategy outcomes, eight tests). Within each family, we performed Holm-Bonferroni P value adjustment for multiple comparisons (*51*). For all families, the significance level was 0.05.

To compare preference and precision outcomes between the knowledgeable and naive cohorts, we used two-tailed t tests. The t tests were conducted using the eight preference-identification trials performed at 1.2 m/s for both cohorts. As before, we performed Holm-Bonferroni P value adjustment within families (preference outcomes, two statistical tests; precision outcomes, two tests). For both families, the significance level was 0.05. All statistical analyses were performed using MATLAB (MathWorks, Natick, MA).

SUPPLEMENTARY MATERIALS

www.science.org/doi/10.1126/scirobotics.abj3487
Materials and Methods
Supplementary Text
Figs. S1 to S13
Tables S1 to S3
Dataset S1

REFERENCES AND NOTES

1. J. Kim, G. Lee, R. Heimgartner, D. A. Revi, N. Karavas, D. Nathanson, I. Galiana, A. Eckert-Erdheim, P. Murphy, D. Perry, N. Menard, D. K. Choe, P. Malcolm, C. J. Walsh, Reducing the metabolic rate of walking and running with a versatile, portable exosuit. *Science* **365**, 668–672 (2019).
2. L. M. Mooney, E. J. Rouse, H. Herr, Autonomous exoskeleton reduces metabolic cost of human walking. *J. Neuroeng. Rehabil.* **11**, 80 (2014).
3. G. Lv, H. Zhu, R. D. Gregg, On the design and control of highly backdrivable lower-limb exoskeletons: A discussion of past and ongoing work. *IEEE Control. Syst.* **38**, 88–113 (2018).
4. G. S. Sawicki, O. N. Beck, I. Kang, A. J. Young, The exoskeleton expansion: Improving walking and running economy. *J. Neuroeng. Rehabil.* **17**, 25 (2020).
5. B. T. Quinlivan, S. Lee, P. Malcolm, D. M. Rossi, M. Grimmer, C. J. Siviy, N. Karavas, D. Wagner, A. T. Asbeck, I. Galiana, C. J. Walsh, Assistance magnitude versus metabolic cost reductions for a tethered multiarticular soft exosuit. *Sci. Robot.* **2**, eaah4416 (2017).
6. J. R. Koller, C. D. Remy, D. P. Ferris, Biomechanics and energetics of walking in powered ankle exoskeletons using myoelectric control versus mechanically intrinsic control. *J. Neuroeng. Rehabil.* **15**, 42 (2018).
7. R. W. Jackson, S. H. Collins, An experimental comparison of the relative benefits of work and torque assistance in ankle exoskeletons. *J. Appl. Physiol.* **119**, 541–557 (2015).
8. P. Malcolm, W. Derave, S. Galle, D. De Clercq, A simple exoskeleton that assists plantarflexion can reduce the metabolic cost of human walking. *PLOS ONE* **8**, e56137 (2013).
9. S. Galle, P. Malcolm, S. H. Collins, D. De Clercq, Reducing the metabolic cost of walking with an ankle exoskeleton: Interaction between actuation timing and power. *J. Neuroeng. Rehabil.* **14**, 35 (2017).
10. J. R. Koller, D. A. Jacobs, D. P. Ferris, C. D. Remy, Learning to walk with an adaptive gain proportional myoelectric controller for a robotic ankle exoskeleton. *J. Neuroeng. Rehabil.* **12**, 97 (2015).
11. A. J. Young, J. Foss, H. Gannon, D. P. Ferris, Influence of power delivery timing on the energetics and biomechanics of humans wearing a hip exoskeleton. *Front. Bioeng. Biotechnol.* **5**, 4 (2017).
12. R. W. Jackson, S. H. Collins, Heuristic-based ankle exoskeleton control for co-adaptive assistance of human locomotion. *IEEE Trans. Neural Syst. Rehabil. Eng.* **27**, 2059–2069 (2019).
13. J. Zhang, P. Fiers, K. A. Witte, R. W. Jackson, K. L. Poggensee, C. G. Atkeson, S. H. Collins, Human-in-the-loop optimization of exoskeleton assistance during walking. *Science* **356**, 1280–1284 (2017).
14. W. Felt, J. C. Selinger, J. M. Donelan, C. D. Remy, "Body-in-the-loop": Optimizing device parameters using measures of instantaneous energetic cost. *PLOS ONE* **10**, e0135342 (2015).
15. J. R. Koller, D. H. Gates, D. P. Ferris, C. D. Remy, "Body-in-the-loop" optimization of assistive robotic devices: A validation study, in *2016 Robotics: Science and Systems* (RSS, 2016), pp. 1–10.
16. Y. Ding, M. Kim, S. Kuindersma, C. J. Walsh, Human-in-the-loop optimization of hip assistance with a soft exosuit during walking. *Sci. Robot.* **3**, eaar5438 (2018).
17. M. Kim, Y. Ding, P. Malcolm, J. Speeckaert, C. J. Siviy, C. J. Walsh, S. Kuindersma, Human-in-the-loop Bayesian optimization of wearable device parameters. *PLOS ONE* **12**, e0184054 (2017).
18. J. C. Selinger, J. M. Donelan, Estimating instantaneous energetic cost during non-steady state gait. *J. Appl. Physiol.* **117**, 1406–1415 (2014).
19. P. Beckerle, G. Salvietti, R. Unal, D. Prattichizzo, S. Rossi, C. Castellini, S. Hirche, S. Endo, H. Ben Amor, M. Ciocarlie, F. Mastrogiovanni, B. D. Argall, M. Bianchi, A human-robot interaction perspective on assistive and rehabilitation robotics. *Front. Neurorobot.* **11**, 24 (2017).
20. D. Gopinath, S. Jain, B. D. Argall, Human-in-the-loop optimization of shared autonomy in assistive robotics. *IEEE Robot. Autom. Lett.* **2**, 247–254 (2017).
21. A. Erdogan, B. D. Argall, Prediction of user preference over shared-control paradigms for a robotic wheelchair, in *Proceedings of the 15th IEEE International Conference on Rehabilitation Robotics (ICORR)* (IEEE, 2017), pp. 1106–1111.
22. D. J. Kim, R. Hazlett-Knudsen, H. Culver-Godfrey, G. Rucks, T. Cunningham, D. Portée, J. Bricout, Z. Wang, A. Behal, How autonomy impacts performance and satisfaction: Results from a study with spinal cord injured subjects using an assistive robot. *IEEE Trans. Syst. Man Cybern. Part A.* **42**, 2–14 (2012).
23. S. Jain, A. Farshchiansadegh, A. Broad, F. Abdollahi, F. Mussa-Ivaldi, B. D. Argall, Assistive robotic manipulation through shared autonomy and a body-machine interface, in *Proceedings of the 14th IEEE International Conference on Rehabilitation Robotics (ICORR)* (IEEE, 2015), pp. 526–531.
24. M. K. Shepherd, E. J. Rouse, Comparing preference of ankle–foot stiffness in below-knee amputees and prosthetists. *Sci. Rep.* **10**, 16067 (2020).
25. M. K. Shepherd, A. M. Simon, J. Zisk, L. J. Hargrove, Patient-preferred prosthetic ankle-foot alignment for ramps and level-ground walking. *IEEE Trans. Neural Syst. Rehabil. Eng.* **29**, 52–59 (2021).
26. M. K. Shepherd, A. F. Azocar, M. J. Major, E. J. Rouse, Amputee perception of prosthetic ankle stiffness during locomotion. *J. Neuroeng. Rehabil.* **15**, 99 (2018).
27. T. R. Clites, M. K. Shepherd, K. A. Ingraham, E. J. Rouse, Patient preference in the selection of prosthetic joint stiffness, in *Proceedings of the 8th IEEE RAS/EMBS International Conference for Biomedical Robotics and Biomechatronics (BioRob)* (IEEE, 2020), pp. 1073–1079.
28. J. M. Caputo, thesis, Carnegie Mellon University (2015).
29. N. Thatte, H. Duan, H. Geyer, A sample-efficient black-box optimizer to train policies for human-in-the-loop systems with user preferences. *IEEE Robot. Autom. Lett.* **2**, 993–1000 (2017).
30. T. R. Clites, M. K. Shepherd, K. A. Ingraham, L. Wontorcik, E. J. Rouse, Understanding patient preference in prosthetic ankle stiffness. *J. Neuroeng. Rehabil.* **18**, 128 (2021).
31. M. Tucker, E. Novoseller, C. Kann, Y. Sui, Y. Yue, J. W. Burdick, A. D. Ames, Preference-based learning for exoskeleton gait optimization, in *2020 IEEE International Conference on Robotics and Automation (ICRA)* (IEEE, 2020), pp. 2351–2357.
32. M. Tucker, M. Cheng, E. Novoseller, R. Cheng, Y. Yue, J. W. Burdick, A. D. Ames, Human preference-based learning for high-dimensional optimization of exoskeleton walking gaits, in *Proceedings of the IEEE/RSJ International Conference on Intelligent Robots and Systems (IROS)* (IEEE, 2021), pp. 3423–3430.
33. K. Li, M. Tucker, E. Bıyık, E. Novoseller, J. W. Burdick, Y. Sui, D. Sadigh, Y. Yue, A. D. Ames, ROIAL: Region of interest active learning for characterizing exoskeleton gait preference landscapes, in *IEEE International Conference on Robotics and Automation (ICRA)* (IEEE, 2021), pp. 3212–3218.
34. K. A. Ingraham, C. D. Remy, E. J. Rouse, User preference of applied torque characteristics for bilateral powered ankle exoskeletons, in *8th IEEE RAS/EMBS International Conference for Biomedical Robotics and Biomechatronics (BioRob)* (IEEE, 2020), pp. 839–845.
35. J. Camargo, A. Ramanathan, W. Flanagan, A. Young, A comprehensive, open-source dataset of lower limb biomechanics in multiple conditions of stairs, ramps, and level-ground ambulation and transitions. *J. Biomech.* **119**, 110320 (2021).
36. E. Reznick, K. R. Embry, R. Neuman, E. Bolívar-Nieto, N. P. Fey, R. D. Gregg, Lower-limb kinematics and kinetics during continuously varying human locomotion. *Sci. Data* **8**, 1–12 (2021).
37. D. A. Winter, Biomechanics of normal and pathological gait: Implications for understanding human locomotor control. *J. Mot. Behav.* **21**, 337–355 (1989).

38. L. M. Mooney, H. Herr, Biomechanical walking mechanisms underlying the metabolic reduction caused by an autonomous exoskeleton. *J. Neuroeng. Rehabil.* **13**, 4 (2016).
39. F. A. Panizzolo, I. Galiana, A. T. Asbeck, C. J. Siviy, K. Schmidt, K. G. Holt, C. J. Walsh, A biologically-inspired multi-joint soft exosuit that can reduce the energy cost of loaded walking. *J. Neuroeng. Rehabil.* **13**, 43 (2016).
40. J. A. Norris, A. P. Marsh, K. P. Granata, S. D. Ross, Positive feedback in powered exoskeletons: Improved metabolic efficiency at the cost of reduced stability?, in *ASME 2007 International Design Engineering Technical Conferences and Computers and Information in Engineering Conference* (ASME, 2007), pp. 1619–1626.
41. P. Antonellis, S. Galle, D. De Clercq, P. Malcolm, Altering gait variability with an ankle exoskeleton. *PLOS ONE* **13**, e0205088 (2018).
42. K. E. Gordon, D. P. Ferris, Learning to walk with a robotic ankle exoskeleton. *J. Biomech.* **40**, 2636–2644 (2007).
43. S. M. Cain, K. E. Gordon, D. P. Ferris, Locomotor adaptation to a powered ankle-foot orthosis depends on control method. *J. Neuroeng. Rehabil.* **4**, 48 (2007).
44. B. F. Mentiplay, M. Banky, R. A. Clark, M. B. Kahn, G. Williams, Lower limb angular velocity during walking at various speeds. *Gait Posture* **65**, 190–196 (2018).
45. U. H. Lee, C. W. Pan, E. J. Rouse, Empirical characterization of a high-performance exterior-rotor type brushless DC motor and drive, in *Proceedings of the IEEE/RSJ International Conference on Intelligent Robots and Systems (IROS)* (IEEE, 2019), pp. 8018–8025.
46. R. G. Budynas, J. K. Nisbett, *Shigley's Mechanical Engineering Design* (McGraw-Hill, ed. 9, 2011).
47. J. Wang, X. Li, T. H. Huang, S. Yu, Y. Li, T. Chen, A. Carriero, M. Oh-Park, H. Su, Comfort-centered design of a lightweight and backdrivable knee exoskeleton. *IEEE Robot. Autom. Lett.* **3**, 4265–4272 (2018).
48. H. Zhu, C. Nesler, N. Divekar, V. Peddinti, R. Gregg, Design principles for compact, backdrivable actuation in partial-assist powered knee orthoses. *IEEE/ASME Trans. Mechatron.* **26**, 3104–3115 (2021).
49. T. Elery, S. Rezazadeh, C. Nesler, R. D. Gregg, Design and validation of a powered knee-ankle prosthesis with high-torque, low-impedance actuators. *IEEE Trans. Robot.* **36**, 1649–1668 (2020).
50. J. Jiang, T. Ngyuen, *Springer Series in Statistics Linear and Generalized Linear Mixed Models and Their Applications* (Springer, ed. 2, 2007).
51. S. Holm, A simple sequentially rejective multiple test procedure. *Scand. J. Stat.* **6**, 65–70 (1979).

Acknowledgments: We wish to acknowledge J. Henderson for statistical advisement and T. Clites for feedback during manuscript preparations. **Funding:** This work is supported, in part, by the NSF grant no. 1256260. Any opinions, findings, and conclusions or recommendations expressed in this material are those of the authors and do not necessarily reflect the views of the NSF. This work was also supported by the D. Dan and Betty Kahn Foundation. Additional funding for C.D.R. was provided by the Carl Zeiss Foundation. **Author contributions:** K.A.I., C.D.R., and E.J.R. were responsible for study conception and design of methodology. K.A.I. collected all experimental data, performed data analyses, and prepared the original draft of this manuscript. K.A.I., C.D.R., and E.J.R. reviewed, edited, and prepared the final manuscript. **Competing interests:** E.J.R. is an inventor on a patent that has been licensed by Dephy Inc. **Data and materials availability:** All data needed to evaluate the conclusions of the paper are available in the paper or the Supplementary Materials.

Submitted 7 May 2021
Accepted 4 March 2022
Published 30 March 2022
10.1126/scirobotics.abj3487

Science Robotics

The role of user preference in the customized control of robotic exoskeletons

K. A. Ingraham, C. D. Remy, and E. J. Rouse

Sci. Robot. **7** (64), eabj3487. DOI: 10.1126/scirobotics.abj3487

Science Robotics (ISSN 2470-9476) is published by the American Association for the Advancement of Science. 1200 New York Avenue NW, Washington, DC 20005. The title *Science Robotics* is a registered trademark of AAAS.